


 Cite this: *RSC Adv.*, 2022, **12**, 13826

## Thiosemicarbazide functionalized carbon quantum dots as a fluorescent probe for the determination of some oxicams: application to dosage forms and biological fluids<sup>†</sup>

Mona E. El Sharkasy, \* Manar M. Tolba, Fathalla Belal, Mohamed I. Walash and Rasha Aboshabana

In this study, highly fluorescent water-soluble nitrogen and sulfur doped carbon quantum dots (N, S-CQDs) were synthesized *via* a one-step hydrothermal process utilizing citric acid as a carbon source and thiosemicarbazide as a sulfur and nitrogen source. The obtained N, S-CQDs exhibited an intense emission band at 415 nm ( $\lambda_{\text{ex}} = 345$  nm). In the presence of either piroxicam, tenoxicam or lornoxicam, the emission band at 415 nm was significantly quenched which might be triggered due to destruction of the surface passivation layer of the N, S-CQDs. A linear correlation was found between the reduction in the fluorescence intensity of N, S-CQDs and the concentration of each drug in the ranges of 2.0–25.0  $\mu\text{M}$ , 10.0–100.0  $\mu\text{M}$  and 20.0–200.0  $\mu\text{M}$  with correlation coefficients of more than 0.999 for all drugs. The detection limits were 0.49  $\mu\text{M}$ , 1.58  $\mu\text{M}$  and 4.63  $\mu\text{M}$  for piroxicam, tenoxicam and lornoxicam, respectively. The effect of experimental parameters affecting the performance of the method was investigated and optimized. The developed sensor has the advantages of simplicity, time-saving, convenience and satisfactory selectivity for determination of the studied drugs in dosage forms with high % recoveries (98.86–101.69%). The method was extended for determination of piroxicam in spiked plasma with % recoveries ranging from 97.95–101.36%. The method was validated in accordance with International Council of Harmonization (ICH) standards, and the results obtained were compared statistically to those given by reported methods, indicating no significant differences in the level of accuracy and precision. The mechanism of the quenching process was studied and elucidated. The structure–activity relationship between the three drugs and the quenching efficiency was also studied and discussed.

 Received 16th February 2022  
 Accepted 25th April 2022

 DOI: 10.1039/d2ra01040b  
[rsc.li/rsc-advances](http://rsc.li/rsc-advances)

### 1. Introduction

Carbon quantum dots (CQDs) have acquired a lot of interest and emerged to be impressive fluorescent nanomaterials with sizes ranging from 2 to 10 nanometers. There are various attributes to this class including inherent fluorescence properties, simplicity and cost-effective synthesis pathways, inexpensive and readily available starting materials, a broad variety of precursor choices, water solubility, excellent biocompatibility, chemical inertness, and ease of functionalization.<sup>1</sup> The solubility of CQDs in aqueous solution may result from the presence of oxygen-containing moieties, such as hydroxyl and carboxyl, on their surfaces. These surface groups may impact the fluorescence characteristics of CQDs.<sup>1</sup> Moreover, the structure of

CQDs consists of  $\text{sp}^2/\text{sp}^3$  carbon and oxygen/nitrogen-based groups or polymeric aggregations.<sup>2</sup> There are numerous forms of fluorescent CQDs such as polymer dots (PDs),<sup>3</sup> carbon nanotube (CNT) dots,<sup>4</sup> graphene quantum dots (GQDs),<sup>5</sup> and nano diamonds (NDs),<sup>6</sup> all have been synthesized so far.

The quantum confinement of the  $\text{sp}^2$ -carbon-constructed core is assumed to be the cause of CQD fluorescence. Heteroatoms may have an effect on CQDs' overall electrical distribution as well as related electronic energy levels. It has been demonstrated that, doping exogenous atoms into CQDs is a successful means of tuning their fluorescence and other properties. Different heteroatoms have been doped into CQDs to enhance their characteristics for promising studies, including sulfur, halogen, nitrogen, silicon, tellurium, boron, selenium and phosphorus.<sup>7,8</sup> Surface functionalization and chemical heteroatoms doping are two valuable ways for increasing photoluminescence efficiency.<sup>9–11</sup> As a result, many scientists have focused their efforts on these species, especially those containing sulfur and nitrogen atoms.<sup>12</sup> Furthermore,

Department of Pharmaceutical Analytical Chemistry, Faculty of Pharmacy, Mansoura University, 35516, Mansoura, Egypt. E-mail: [MonaElsharkasy524@gmail.com](mailto:MonaElsharkasy524@gmail.com)

† Electronic supplementary information (ESI) available. See <https://doi.org/10.1039/d2ra01040b>



doping non-metallic elements into CQDs allows for structural and compositional changes, as well as a variety of benefits over heavy metal-based semiconductor-based QDs.<sup>12</sup>

CQDs can be synthesized using two alternative ways, top-down and bottom-up methods. The method of slicing large carbon containing compounds into small fragments and modifying oxygen-based groups is referred to top-down method. This method generally produces CQD with homogenous particle sizes and controllable surface chemistry.<sup>7</sup> While, bottom-up methods are better in performance and can be used to produce CQDs in wide scale. Most approaches may result in dehydration and subsequent carbonization of molecules and polymers, resulting in CQDs or PDs formation. CQDs produced *via* "bottom-up" approach often include a significant number of functional groups that can be subsequently functionalized,<sup>13</sup> but they also have a wide size range, necessitating extensive purification and extraction methods. The literature has shown several methods for producing N, S-CQDs probe, including hydrothermal approaches utilizing citric acid and cysteine<sup>12,14</sup> or cystamine dihydrochloride,<sup>15</sup> microwave-assisted methods,<sup>16</sup> carbonizing organics methods<sup>17</sup> and chemical oxidation methods.<sup>18</sup> Most of these techniques, however, were impractical due to the need for lengthy procedures or expensive equipment. As a result, developing a cost-effective procedure using readily available starting material was needed.

Oxicams including piroxicam (PRX), tenoxicam (TNX) and lornoxicam (LRX), are enolic acids, that inhibit cyclooxygenase enzymes (COX-1 and COX-2), having analgesic, antipyretic and anti-inflammatory activities.<sup>19</sup> They differ from non-steroidal anti-inflammatory drugs (NSAIDs) derived from carboxylic acids, which have a short half-life, and hence require frequent daily administration.<sup>20</sup>

Piroxicam (PRX, Fig. 1a), chemically is 4-hydroxy-2-methyl-N-2-pyridinyl-2H-1,2-benzothiazine-3-carboxamide 1,1-dioxide. Since PRX is acidic and lipophilic compound, it can be quickly absorbed and widely distributed across the body, reaching significant blood levels within one to two hours.<sup>20,21</sup> PRX, like other NSAIDs, inhibits COX enzyme, which is involved in the pathogenesis of primary dysmenorrhea. PRX is also used to treat acute musculoskeletal pain, acute gout, rheumatoid arthritis, osteoarthritis, postsurgical and posttraumatic pain. The recommended dose in these acute painful conditions is

40 mg while for chronic conditions is 20 mg once a day.<sup>20</sup> For PRX determination, a variety of approaches have been reported including spectrophotometry,<sup>22-25</sup> spectrofluorimetry,<sup>26,27</sup> HPLC,<sup>22,28</sup> electrochemical methods<sup>29,30</sup> and capillary electrophoresis.<sup>31,32</sup>

Tenoxicam (TNX, Fig. 1b), is a thiophene derivative, chemically named 4-hydroxy-2-methyl-N-(2-pyridyl)-2H-thieno[2,3-e] [1,2]thiazine-3-carboxamide1,1-dioxide. Various methods for analysis of TNX have been reported, including spectrophotometry,<sup>24,25,33,34</sup> spectrofluorimetry,<sup>35</sup> HPLC<sup>34,36,37</sup> and electrochemical methods.<sup>38,39</sup> The structure of lornoxicam (LRX, Fig. 1c) is (6-chloro-4-hydroxy-2-methyl-N-2-pyridyl-2H-thieno[2,3-e]-1, 2-thiazine-3-carboxamide-1,1-dioxide). LRX can be administered orally or intravenously. It differs from other oxicams in that, it has a short elimination half-life (3 to 5 hours), which can be beneficial in terms of tolerability.<sup>40</sup> Variable methods were reported for determination of LRX including spectrophotometry,<sup>33,41</sup> spectrofluorimetry,<sup>35</sup> HPLC,<sup>42-44</sup> and electrochemical methods.<sup>45,46</sup> The previously reported methods require expensive instrumentation, tedious and time-consuming procedures.

In this study, an eco-friendly N, S-CQDs were synthesized from citric acid and thiosemicarbazide. The main objective of the current study was applying N, S-CQDs as fluorescent probe to determine each of PRX, TNX, and LRX in various dosage forms and/or biological samples. Despite the fact that the selected pharmaceuticals have particular groups that alter their fluorimetric determination, the majority of the literature is based on using of strong acid such as nitric acid or reactions with chromogenic reagent of time-consuming procedure. Therefore, the proposed method introduced a simple, fast, green and direct spectrofluorimetric method for their determination in dosage forms and/or biological samples for the first time without a need for pre-derivatization steps.

## 2. Experimental section

### 2.1. Reagents and materials

All chemicals used were of Analytical Reagent grade, and the solvents were of HPLC grade.

- Piroxicam pure sample (PRX) was kindly supplied by Pharco Pharmaceuticals Co., Amriya, Alexandria, Egypt.

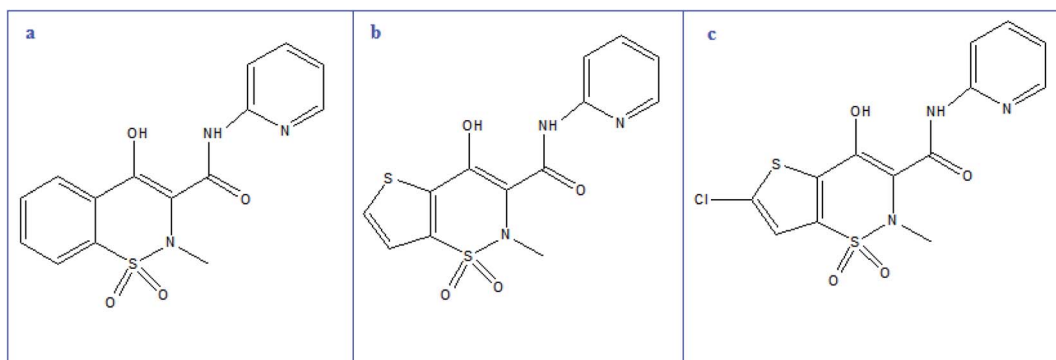


Fig. 1 Structural formula of PRX (a), TNX (b) and LRX (c).



- Tenoxicam pure sample (TNX) was supplied by the Egyptian International Pharmaceutical Industries Co. EIPICO, 10<sup>th</sup> of Ramadan City, Industrial Zone B1, Egypt.

- Lornoxicam pure sample (LRX) was supplied by El Obour Modern Pharmaceutical Industries Co., 1<sup>st</sup> Industrial Zone Obour City, Kaliobeya, Egypt.

- Pharmaceutical formulations:

- ❖ Feldene® 20 mg tablets; batch #20401, Feldene® 20 mg capsules; batch #20303 and Feldene® 20 mg ampoules; batch #200220020 manufactured by Pfizer Egypt S.A.E, Cairo A.R.E. Under license of Pfizer Inc., USA.

- ❖ Tenoxicam® 20 mg capsules; batch #145070, Epicotil® 20 mg ampoules; batch #2006576, product of El Obour Modern Pharmaceutical Industries co., 1<sup>st</sup> Industrial Zone Obour City, Kaliobeya, Egypt.

- ❖ Lornicam® Rapid 8 mg tablets; batch #201583, product of El Mira International for Pharmaceuticals and Chemicals, Nasr City, Cairo, Egypt.

- ❖ Lornoxicam® 8 mg ampoules; batch #20026048, product of Global Pharmaceutical Industries, 5<sup>th</sup> Industrial Zone, 6<sup>th</sup> of October City, Egypt.

- Phosphoric acid, boric acid, sodium hydroxide, citric acid (CA), thiosemicarbazide (TSC), and methanol were purchased from Sigma-Aldrich (USA).

- Membrane filters with pore sizes of 0.45  $\mu\text{m}$  (Phenomenex - USA).

- Mansoura University Hospitals (Mansoura, Egypt) gratefully supplied human plasma samples, which were maintained frozen till use following gentle thawing.

- Throughout the experiments, double distilled water was utilized.

## 2.2. Standard stock solutions and buffer solution

- A stock solution (1.0 mM) of PRX was prepared in a 100 mL volumetric flask by dissolving 0.033 g of PRX in 5 mL dimethyl sulphoxide (DMSO) and completing to 100 mL with ethanol.

- TNX and LRX stock solutions of concentration of 1.0 mM were prepared separately in 100 mL volumetric flasks by dissolving 0.0337 g and 0.0371 g, respectively in double distilled water. Working solutions were prepared by diluting standard stock solutions as appropriate.

- Britton-Robinson buffer solutions were prepared by mixing 0.04 M of each of acetic acid, boric acid and phosphoric acid. The required pH of buffer solution was adjusted using 0.2 M sodium hydroxide to obtain different buffer solutions with pH range 2.0–12.0.

## 2.3. Synthesis of fluorescent probe

Synthesis of nano-sensor was performed applying a simple hydrothermal method recently reported in the literature.<sup>47,48</sup> The fluorescent N, S-CQDs probe of concentration of 1.0 g L<sup>-1</sup>, was prepared from CA and TSC as starting materials in a one-step hydrothermal method. The probes were made by sonicating a mixture of TSC (0.68 g, 7.50 mM) and CA (0.52 g, 2.50 mM) in 20.0 mL of double distilled water. The reaction mixture was stirred then refluxed at 160 °C for 8 hours until fluorescent

nano-sensor was produced. The mixture was then allowed to cool before incubation at room temperature for subsequent use.

## 2.4. Instrumentation

**2.4.1. For fluorescence measurements.** Cary Eclipse Fluorescence spectrophotometer with a xenon flash lamp from Agilent Technologies (Santa Clara, CA 95051, United States). Slit width was adjusted at 5 nm and the instrument's sensitivity was set at 800 V.

**2.4.2. For spectrophotometric measurements.** The spectrophotometer utilized in the study was UV-vis spectrophotometer (UV-1601 PC, Shimadzu, Kyoto, Japan).

**2.4.3. For identification of FT-IR spectra.** Thermo Fisher Scientific infrared spectrometer (The Nicolet – iS10 FT-IR, 168 Third Avenue Waltham, MA, USA) was utilized for characterization of the obtained dots in the range of 4000 to 1000 cm<sup>-1</sup> with a resolution of 4 cm<sup>-1</sup>.

**2.4.4. For characterization of N, S-CQDs.** At 200 kV, the JEM-2100 high-resolution transmission electron microscope (HRTEM) was used (JEOL, Tokyo).

**2.4.5. For monitoring the temperature.** Water bath of England Cambridge Ltd. Shaker was used.

**2.4.6. For sonication and mixing.** Ultrasonic bath, model SS 101 H 230, (USA).

**2.4.7. For measuring and regulating of pH.** A Consort NV P-901 Belgium pH meter was used.

## 2.5. Procedures

**2.5.1. Calibration graphs.** Aliquots of PRX, TNX or LRX standard solutions covering the working concentration ranges were transferred into a series of 10 mL volumetric flasks. Then 0.25 mL aliquots of the fluorescent probe were added and volumes were completed to the mark with distilled water and thoroughly mixed. The fluorescence intensities of the emission bands were measured at 415 nm ( $\lambda_{\text{ex}} = 345$  nm). In the same time, a blank solution was prepared and measured. The calibration curves were constructed by plotting the quenching values of fluorescence ( $\Delta F$ ) against final drug concentrations in  $\mu\text{M}$  and the corresponding regression equations were then derived.

### 2.5.2. Procedure for dosage forms

#### 2.5.2.1. For determination of PRX

**2.5.2.1.a. In Feldene® tablets and capsules.** Ten tablets were separately grinded, well-mixed and weighed. Ten capsules were evacuated and weighed. An accurately weighed amount of the powder of each preparation equivalent to 0.033 g of PRX was transferred into a small conical flask, 5 mL aliquot of DMSO was added and mixed, and then 50 mL of ethanol was added and sonicated for 30 minutes. The resulting solution was filtered into a 100 mL volumetric flask and completed to the mark with ethanol to produce solution of final concentration of 1.0 mM, then serially diluted to reach the working concentration range. The procedure under “Section 2.5.1” was then applied. The nominal contents of the tablets or capsules were obtained using the corresponding regression equation.



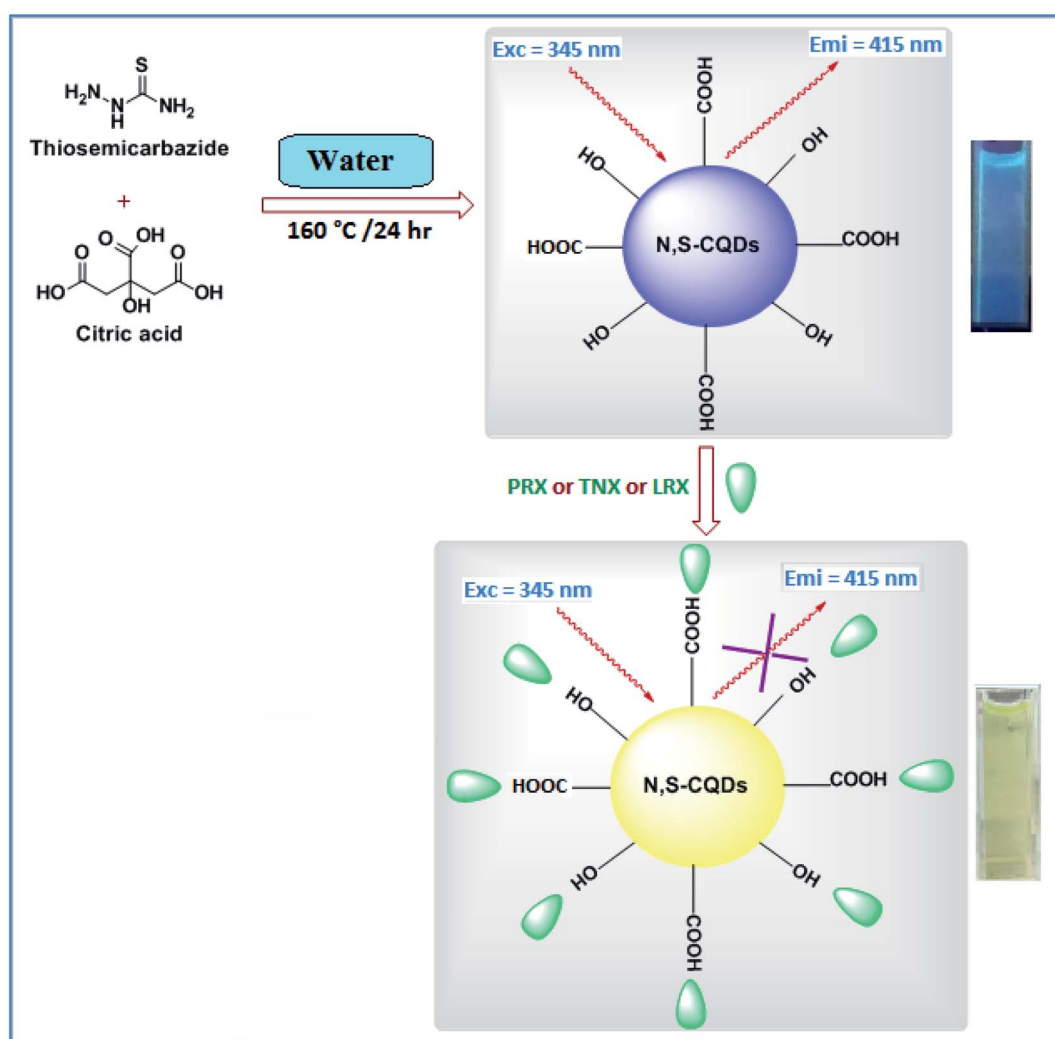
**2.5.2.1.b. In Feldene® ampoules.** The contents of five ampoules were mixed. Accurately measured volume of the mixed solution equivalent to 0.033 g of PRX was transferred into a 100 mL volumetric flask. Then, the volume was completed to the mark with ethanol to obtain a final concentration of 1.0 mM. The solution was then serially diluted to the working concentration range. The procedure under “Section 2.5.1” was then applied and the nominal content of the ampoules was calculated using the corresponding regression equation.

**2.5.2.2. For analysis of TNX and LRX preparations.** Ten tablets of Lornoxicam Rapid® tablets were separately weighed, pulverized and mixed. Ten capsules of Tenoxicam® capsules were evacuated and weighed. An accurately weighed amount of the powder equivalent to 0.0371 g of LRX or 0.0337 g of TNX was transferred separately into 100 mL conical flasks. About 50 mL of double distilled water was added and mixed well, sonicated for 30 minutes, filtered into 100 mL volumetric flasks and completed to the mark with the same solvent to produce solutions of final concentration of 1.0 mM. Proceed as described under “Section 2.5.1”.

For Epicotil® or Lornoxicam® vials, the contents of five vials were homogeneously mixed. An accurately weighed amount of the powder equivalent to 0.0337 of TNX and 0.0371 g of LRX were transferred separately into 100 mL conical flasks, and then about 50 mL of double distilled water was added. Each solution was mixed, sonicated for 30 minutes, filtered into 100 mL volumetric flask and completed to the mark with the same solvent to produce solution of final concentration of 1.0 mM. Serial dilutions were performed and the procedure was completed as described under “Section 2.5.1”. The nominal content of each preparation was calculated using the corresponding regression equation.

### 2.5.3. Analysis of PRX in spiked human plasma sample.

1.0 mL aliquots of human plasma samples were spiked with increasing volumes of PRX standard solution (1.0 mM) and vortex mixed for 1.0 min in centrifugation tubes. Plasma proteins were precipitated by adding ethanol up to 5 mL. After vortex mixing for about 30 seconds, the tubes were centrifuged for about 30 minutes at 3600 rpm, and the clear supernatant was filtered through syringe filters. Then, 1.0 mL aliquots of the filtrate were transferred into a series of 10 mL volumetric flasks,



**Scheme 1** General procedure for hydrothermal synthesis and application of N, S-CQDs.



0.25 mL aliquots of fluorescent sensor were added, and the volume was completed to the mark with distilled water to get final concentration within the linearity range. A blank experiment was run at the same time, and the analysis was carried out as described under "Section 2.5.1". The % recovery was calculated using the corresponding regression equation.

### 3. Results and discussion

#### 3.1. Synthesis and characterization of fluorescent probe

In this method, a green and cost-effective fluorescent probe was produced adopting a hydrothermal technique using CA as a source of carbon to produce carboxyl coated CQDs.<sup>47</sup> The carboxylic groups of the prepared CQDs were then reacted with amine and sulfur groups of TSC to produce TSC functionalized CQDs (Scheme 1). In their native condition, the synthesized N, S-CQDs are extremely water soluble, with no visible precipitation after 14 days at 4 °C.

**3.1.1. High-resolution transmission electron microscope (HRTEM).** The size and morphology of fluorescent probe particles were investigated using HRTEM. In this technique, the samples were mounted onto a carbon-coated Cu-grid of about 200 meshes and analyzed using HRTEM at 200 kV. It was observed that, N, S-CQDs are spherical in shape with diameters ranging from 4.8 to 9.2 nm as demonstrated in Fig. 2.

#### 3.1.2. Spectral characteristic of N, S-CQD

**3.1.2.1. Spectroscopic investigation.** Fig. S1† illustrates the UV-vis absorption spectra of CA, TSC, and N, S-CQDs. It was observed that N, S-CQDs showed an apparent UV-vis absorption peak in the range of 290–360 nm with a maximum at about 310 nm, which is attributable to the trapping of excited-state energy by the surface states, resulting in strong emission.<sup>49,50</sup>

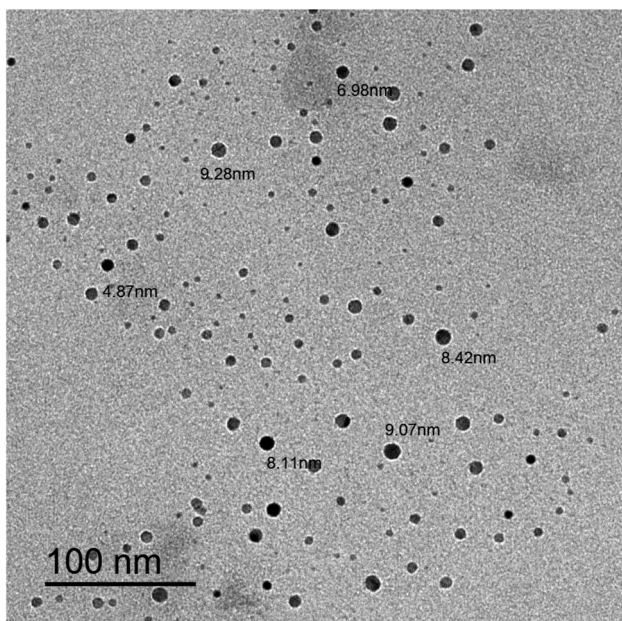


Fig. 2 Typical HRTEM images of the N, S-CQDs.

**3.1.2.2. Fluorimetric investigation.** Fluorescence properties of N, S-CQDs were carefully studied. The fluorescence emission is excitation-dependent in the wavelength range of 310 to 380 nm as illustrated in Fig. 3. This may be resulting from multiple C-, N-, O-, and S-containing functional groups on the surface of N, S-CQDs leading to numerous surface states with varied energy levels and emissive traps.<sup>51</sup> At higher excitation wavelength, it was observed that emission peak spectra were red shifted and the fluorescence intensity decreased. As demonstrated in Fig. S2,† when N, S-CQDs were excited at 345 nm, they emitted fluorescence strongly at around 415 nm.

**3.1.2.3. FT-IR spectroscopic studies.** The hydrophilic functional groups capped on the surface of N, S-CQDs are responsible for their water solubility.<sup>52,53</sup> FT-IR analysis of N, S-CQDs surface show different functional groups<sup>54–57</sup> as illustrated in Fig. 4. All functional heights presented in FT-IR analysis was mentioned in Table 1.

#### 3.2. Fluorescence quenching mechanism

As demonstrated in Scheme 1, adding the investigated drugs to the N, S-CQDs solution significantly decreased the emitted blue fluorescence. This might be due to destruction of the surface passivation layer of N, S-CQDs.<sup>14,47,58</sup> In aqueous solutions, the emission spectra of fluorescent probe were recorded in the absence and presence of various concentrations of PRX, TNX, and LRX. The fluorescence band observed was primarily focused at 415 nm (excitation 345 nm). As shown in Fig. S3,† the fluorescence emission spectra obtained when PRX, TNX, or LRX were added to the probe were significantly decreased. Generally, fluorescence quenching pathways can be classified into two categories: static or dynamic quenching. The temperature dependence of both categories of quenching mechanisms could be used for differentiation.<sup>59,60</sup> Raising the temperature causes the diffusion coefficient, particle mobility, and energy transfer to rise in case of dynamic quenching. As a result, as the temperature increases, the quenching rate constant goes up as well. In a static one, on the other hand, when the temperature rises, the quenching rate constant decreases because the stability of non-fluorescent complex is lowered.<sup>59</sup> The potential quenching

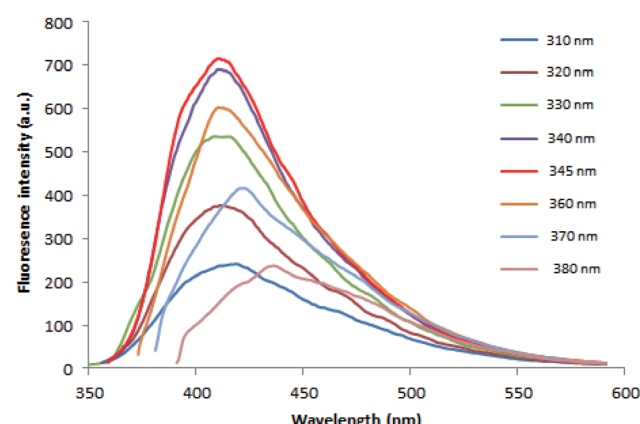


Fig. 3 Fluorescence spectra of the N, S-CQDs at different excitation wavelengths.



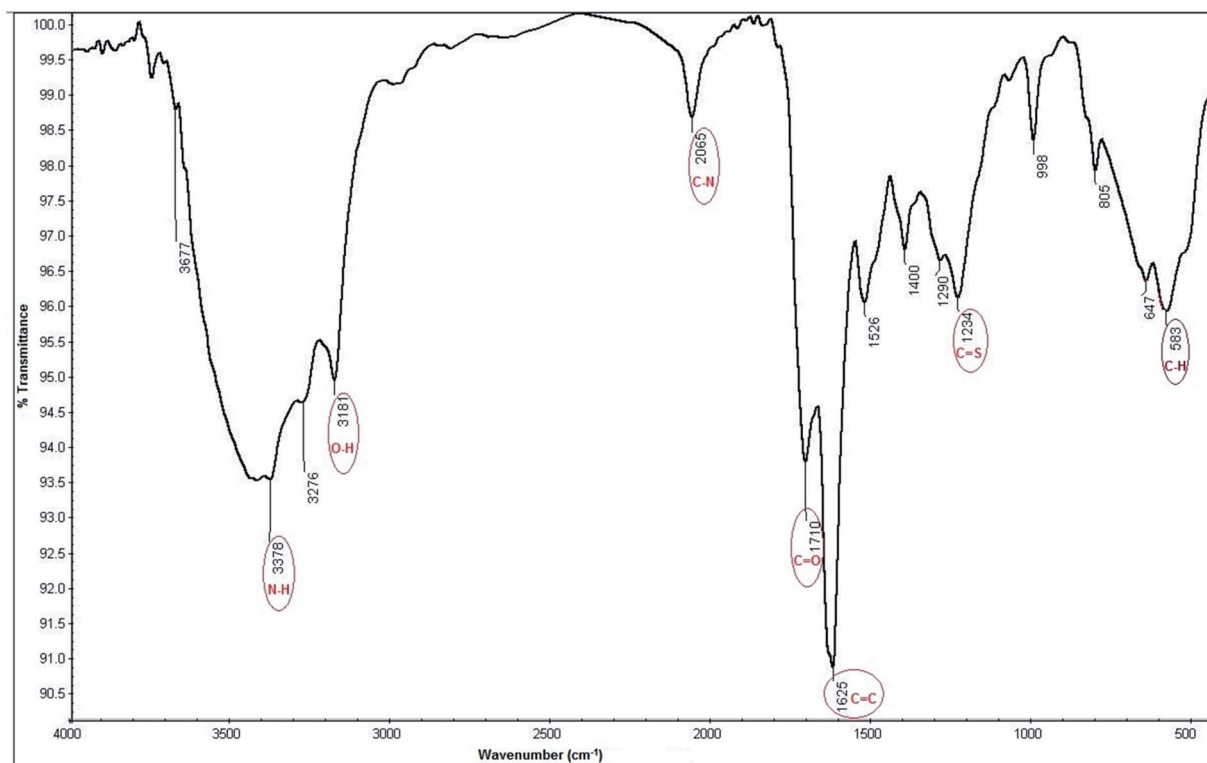


Fig. 4 FT-IR spectra of N, S-CQDs.

Table 1 FT-IR analysis of N, S-CQDs

Functional groups	Wavenumber (cm <sup>-1</sup> )
N-H/O-H	3500–3100
C=O	1710
C-N	2065
C=C	1625
C=S	1234
C-H	583

mechanism can be illustrated by the Stern–Volmer equation, eqn (1).<sup>61</sup>

$$F_0/F = 1 + K_{SV}[Q] \quad (1)$$

$F$  and  $F_0$  are the fluorescence intensities in the presence and absence of PRX, TNX or LRX.  $K_{SV}$  is the Stern–Volmer quenching constant.  $[Q]$  denotes the drug concentration.<sup>61</sup>

The Stern–Volmer plot for fluorescence quenching was conducted at 293, 318 and 353 K between  $F_0/F$  and  $[Q]$ . The plot was linear and the slope ( $K_{SV}$ ) was increased with increasing temperature (Fig. 5), indicating that the quenching process proceeded through dynamic one.<sup>62</sup>

### 3.3. Optimization of variables affecting fluorescence sensing

**3.3.1. Effect of pH.** It is widely understood that the pH of a solution influences not only the fluorescence intensity of N, S-

CQDs, but also the interactions between N, S-CQDs and target species.<sup>63</sup> The effect of pH on the quenching value ( $\Delta F$ ) of fluorescence intensity of N, S-CQDs by PRX, TNX, or LRX was studied using Britton–Robinson buffer with a concentration of 0.2 M over the pH range 2.0–12.0. It was found that changing pH did not significantly affect the fluorescence intensities of the studied drugs as shown in Fig. 6a. As a result, no buffer solution was required in subsequent work, and all experiments were conducted without buffer, adding the advantage of simplicity to the proposed method.

**3.3.2. The influence of the incubation period.** The incubation period was also studied due to its significant effect on fluorescence intensity. It was investigated after the addition of the studied medications to N, S-CQDs. Fluorescence spectra were measured at intervals ranging from one minute to 30 minutes as shown in Fig. 6b. It was observed that the reaction between the investigated drugs and N, S-CQDs was rapid, requiring just one minute to complete and the fluorescence signals remained stable for nearly 30 minutes, giving this method the advantage of time-saving.

### 3.4. Validation of the method

To prove if the proposed approach was valid, the International Conference on Harmonization (ICH) Q2 (R1) guidelines<sup>64</sup> were adopted.

**3.4.1. Linearity and range.** The fluorescence emission spectra of N, S-CQDs with and without the three analytes were recorded after the reaction conditions were optimized, and the

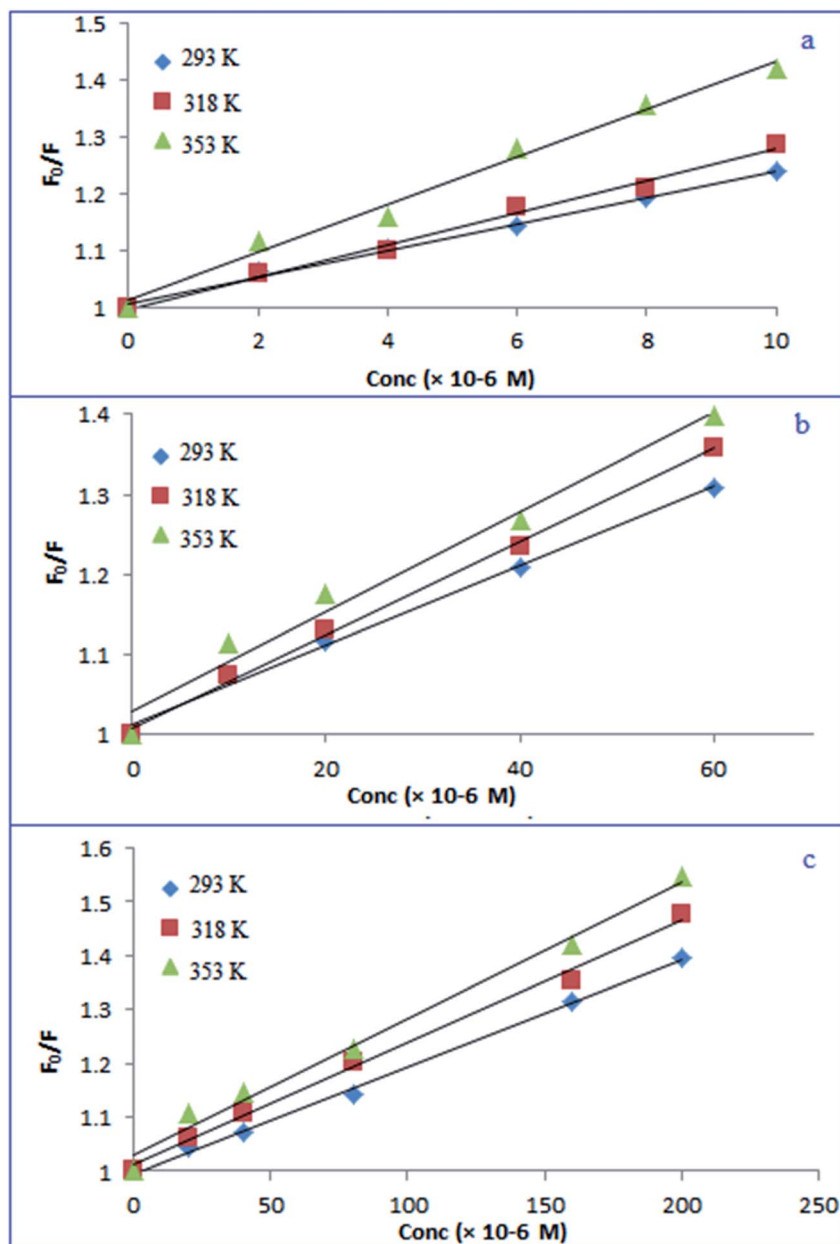


Fig. 5 Stern–Volmer plots of the PRX/TNX/LRX (a–c) – N, S-CQDs at different temperatures.

calibration curves were constructed by plotting the difference in fluorescence intensity ( $\Delta F$ ) versus the final drug concentrations in  $\mu\text{M}$ .

For PRX, TNX, and LRX, the relationship was rectilinear over the ranges of 2.0–25.0  $\mu\text{M}$ , 10.0–100.0  $\mu\text{M}$  and 20.0–200.0  $\mu\text{M}$ , respectively as shown in Fig. S4.† Data abridged in Table 2 show the output results as well as statistical parameters of the data. The results revealed high correlation coefficients with low values of standard deviation of intercept ( $S_a$ ), standard deviation of slope ( $S_b$ ), and residual standard deviation ( $S_{y/x}$ ), implying that the calibration curves are extremely linear and precise.

**3.4.2. Limit of quantitation (LOQ) and limit of detection (LOD).** The LOQ and LOD were determined according to ICH

Q2R1 recommendations,<sup>64</sup> where LOQ was verified by determining the smallest drug concentration that can be quantitatively measured and statistically corresponds to  $10 S_a/b$  and LOD was known as the smallest drug concentration that can be identified by the proposed method and statistically corresponds to  $3.3 S_a/b$  ( $S_a$  is the standard deviation of the intercept &  $b$  is the slope of the calibration curve). Based on the obtained LOD and LOQ values, the suggested method is sufficiently sensitive as illustrated in Table 2.

**3.4.3. Accuracy and precision.** The accuracy of the proposed method was demonstrated by comparing the results of the proposed method in raw materials and pharmaceuticals to the results of the comparison methods.<sup>22,34,41</sup> Data in Table 3 illustrate no significant differences between the performance of

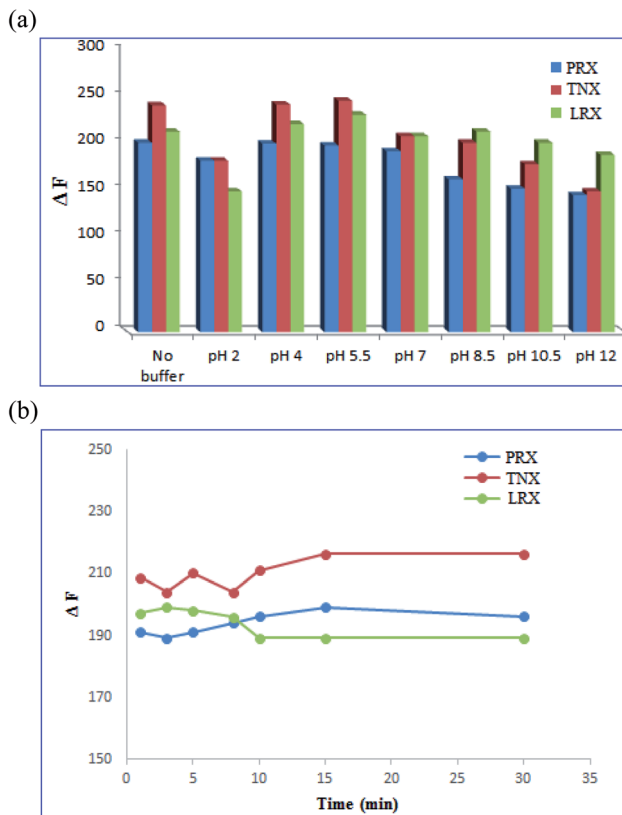


Fig. 6 (a) The effect of pH of the buffer on fluorescence quenching of N, S-CQDs. (b) The effect of incubation time on fluorescence intensity of N, S-CQDs.

Table 2 Analytical performance data for the proposed method

Validation parameter	PRX	TNX	LRX
Linearity range ( $\mu\text{M}$ )	2.0–25.0	10.0–100.0	20.0–200.0
Intercept ( $a$ )	26.082	40.841	7.310
Slope ( $b$ )	15.504	3.106	1.305
Correlation coefficient ( $r$ )	0.9996	0.9999	0.9997
S.D. of residuals ( $S_{y/x}$ )	3.64	1.91	2.36
S.D. of intercept ( $S_a$ )	2.30	1.49	1.83
S.D. of slope ( $S_b$ )	0.17	0.02	0.02
Limit of detection, LOD ( $\mu\text{M}$ )	0.49	1.58	4.63
Limit of quantitation, LOQ ( $\mu\text{M}$ )	1.49	4.78	14.05

the two methods concerning the accuracy and precision. This was confirmed by statistical analysis of the data using Student's *t*-test and variance ratio *F*-test, respectively.<sup>65</sup>

The method's precision was evaluated by determination of intermediate precisions and repeatability. Three distinct concentrations were tested from each compound, each with three replicates. Table 4 shows that the method developed has a reasonable SD and % RSD values of less than 2.0.

**3.4.4. Specificity.** The specificity of the suggested procedure was studied and it was found that common excipients added to ampoules, capsules, and tablets as well as the endogenous component of plasma matrix didn't have any effect

Table 3 Application of the proposed method for the determination of the studied drugs in their raw materials

Parameters	Amount taken ( $\mu\text{M}$ )	Amount found ( $\mu\text{M}$ )	% found <sup>a</sup>	PRX			TNX			LRX		
				Amount taken ( $\mu\text{M}$ )	Amount found ( $\mu\text{M}$ )	% found <sup>a</sup>	Amount taken ( $\mu\text{M}$ )	Amount found ( $\mu\text{M}$ )	% found <sup>a</sup>	Amount taken ( $\mu\text{M}$ )	Amount found ( $\mu\text{M}$ )	% found <sup>a</sup>
2.0	1.962	98.10	10.0	9.874	98.74	20.0	19.754	19.754	98.77	40.0	40.327	100.82
4.0	3.905	97.63	20.0	20.201	101.01	40.0	40.0	40.0	100.36	80.0	79.486	99.36
6.0	6.045	100.75	40.0	40.462	101.16	80.0	59.414	59.414	99.44	120.0	119.325	101.79
8.0	7.941	99.26	60.0	79.628	99.54	160.0	100.44	100.44	99.13	200.0	198.264	99.13
10.0	10.104	101.04	80.0	79.628	99.54	160.0	100.44	100.44	99.13	200.0	198.264	99.13
15.0	15.079	100.53	100.0	100.435	100.44	100.0	100.435	100.435	100.0	200.0	198.264	99.13
20.0	20.348	101.74	101.74	100.435	100.44	100.0	100.435	100.435	100.0	200.0	198.264	99.13
25.0	24.657	98.63	98.63	98.63	98.63	98.63	98.63	98.63	98.63	98.63	98.63	98.63
<b>Mean <math>\pm</math> S.D.</b>	<b>99.71 <math>\pm</math> 1.51</b>						<b>99.99 <math>\pm</math> 1.03</b>					<b>99.89 <math>\pm</math> 1.17</b>
<b>Mean <math>\pm</math> S.D.</b>	<b>99.87 <math>\pm</math> 1.27</b>						<b>99.42 <math>\pm</math> 0.74</b>					<b>101.26 <math>\pm</math> 0.72</b>
$t^b$	0.16 (2.26)						0.82 (2.37)					1.78 (2.37)
$F^b$	1.41 (19.35)						1.94 (19.30)					2.64 (19.30)

<sup>a</sup> Average of 3 replicate determinations. <sup>b</sup> The values between parentheses are the tabulated values of *t* and *F* at *P* = 0.05.<sup>65</sup>

Table 4 Intra-day and inter-day precision data for the studied drugs using the proposed method

Concentration ( $\mu\text{M}$ )	Intra-day precision			Inter-day precision			
	Mean $\pm$ SD	% RSD	% error	Mean $\pm$ SD	% RSD	% error	
PRX	4.0	100.64 $\pm$ 1.42	1.41	0.81	101.11 $\pm$ 1.19	1.18	0.68
	10.0	101.34 $\pm$ 1.24	1.22	0.70	100.65 $\pm$ 1.05	1.04	0.60
	15.0	99.70 $\pm$ 0.31	0.31	0.18	98.12 $\pm$ 1.67	1.70	0.98
TNX	40.0	100.14 $\pm$ 0.89	0.89	0.51	100.46 $\pm$ 1.68	1.67	0.96
	60.0	99.33 $\pm$ 0.95	0.96	0.55	98.85 $\pm$ 0.28	0.28	0.16
	80.0	96.88 $\pm$ 0.14	0.14	0.08	97.78 $\pm$ 1.46	1.49	0.86
LRX	40.0	98.57 $\pm$ 1.30	1.32	0.76	99.91 $\pm$ 0.96	0.96	0.55
	80.0	100.62 $\pm$ 1.42	1.41	0.81	101.58 $\pm$ 1.13	1.11	0.64
	160.0	101.50 $\pm$ 1.34	1.32	0.76	99.83 $\pm$ 1.69	1.69	0.98

Table 5 Application of the proposed method for the determination of PRX, TNX and LRX in their pharmaceutical preparations

Pharmaceutical formulations	Parameters		Comparison methods <sup>22,34,41</sup>	<i>t</i> -Test (2.78) <sup>a</sup>	<i>F</i> -Value (19.00) <sup>a</sup>
	Mean $\pm$ % RSD	<i>N</i>			
Feldene® ampoule (20 mg PRX per amp.)	100.16 $\pm$ 1.81	3.00	99.87 $\pm$ 1.54	0.23	1.38
Feldene® capsule (20 mg PRX per cap.)	98.86 $\pm$ 0.78		99.92 $\pm$ 0.68	1.62	1.32
Feldene® tablet (20 mg PRX per tab.)	101.45 $\pm$ 1.39		100.17 $\pm$ 1.91	0.99	1.89
Epicotil® vial (20 mg TNX per vial)	99.13 $\pm$ 0.33		100.35 $\pm$ 0.74	2.26	5.03
Tenoxicam® capsule (20 mg TNX per cap.)	101.69 $\pm$ 0.43		100.31 $\pm$ 1.30	1.64	9.14
Lornoxicam® vial (8 mg LRX per vial)	99.46 $\pm$ 1.31		101.20 $\pm$ 0.64	1.96	4.19
Lornicam Rapid® tablet (8 mg LRX per tab.)	99.58 $\pm$ 1.76		99.94 $\pm$ 1.37	0.30	1.65

<sup>a</sup> The values between parentheses are the tabulated values of *t* and *F* at *P* = 0.05.<sup>65</sup>

on the fluorescence signals obtained in this study as illustrated in Table 5.

### 3.5. Structure versus activity correlation

Referring to the molecular structure of the three studied compounds, it was noticed that PRX contain benzyl group (non-polar) in its side chain, TNX on the other hand contains thiophene group (polar group because of the presence of sulphur atom) while LRX has chloro-thiophene (more polar group as it contains additional chlorine atom). From the obtained results, it was found that there is a direct correlation between the sensitivity of the proposed method (as measured by LOD values) and the gradual increase of the polarity of the studied drugs. The sensitivity was found to be reduced from PRX to TNX and then LRX with the increase of their polarity which in turn decreases binding interaction with N, S-CQDs.

### 3.6. Method applications

**3.6.1. Pharmaceutical applications.** The developed method was successfully applied to assay PRX, TNX and LRX in their various pharmaceutical formulations. The % recoveries were calculated using the previously derived regression equations. Using the Student's *t*-test and the variance ratio *F*-test,<sup>65</sup> the results obtained were compared to those of reported methods.<sup>22,34,41</sup> According to the calculated *t* and *F* values,<sup>65</sup>

there is no considerable difference between the methods in terms of accuracy and precision, respectively as shown in Table 5.

### 3.6.2. Analysis of PRX in spiked human plasma samples.

The basic goal of method validation is to verify that a particular

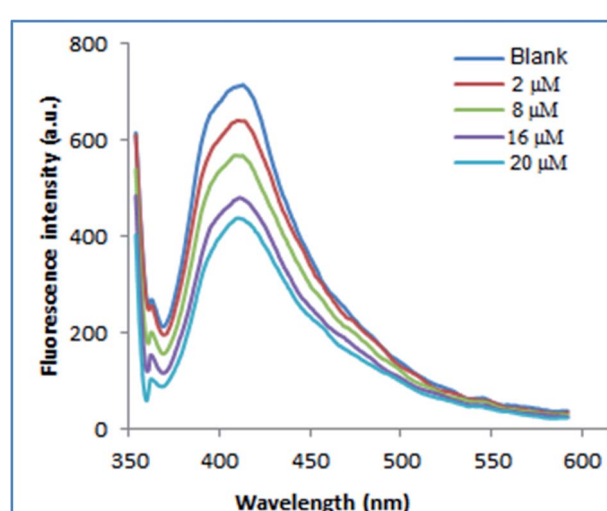


Fig. 7 Application of proposed method for determination of PRX in spiked human plasma.



Table 6 Application of the proposed method for determination of PRX in spiked human plasma

Parameters	Amount taken (μM)	Amount found (μM)	% recovery
	2.0	1.956	97.95
	8.0	8.114	101.36
	16.0	16.101	100.47
	20.0	19.869	99.46
Mean ± S.D.			99.81 ± 1.46
Regression equation	$y = 11.3587x + 54.3497$		
<i>r</i>	0.9998		
S.D. of residuals ( $S_{y/x}$ )	2.23		
S.D. of intercept ( $S_a$ )	2.15		
S.D. of slope ( $S_b$ )	0.16		
Limit of detection, LOD (μM)	0.62		
Limit of quantitation, LOQ (μM)	1.89		

procedure for determining an analyte concentration in a certain biological matrix, such as blood, plasma, serum urine, or saliva, is reliable. Piroxicam is quickly absorbed following oral or rectal administration. In urine, around 10% of oral dose is eliminated unchanged. Repeated administration of PRX causes it to accumulate in the body.<sup>66</sup> The therapeutic level is normally between 5 and 10 mg L<sup>-1</sup>. Maximum steady-state plasma concentrations of 2.1 to 4.3 (mean 3.2), 3.6 to 6.5 (mean 4.5), and 9.0 to 16.5 (mean 11.7) mg L<sup>-1</sup> were reported after daily oral administration of 10, 20, and 30 mg to 5 subjects.<sup>66,67</sup> The proposed method was efficiently applied to determine PRX in spiked human plasma sample (Fig. 7). The regression equation in urine was  $y = 11.36X + 54.35$ , where:  $y$  is the difference in FI,  $X$  is the concentration of PRX.

The % recoveries ranged from 97.95 to 101.36 as represented in Table 6.

## 4. Conclusion

Based on the quenching of the fluorescence of N, S-CQDs, a novel methodology for analysis of PRX, TNX and LRX in different dosage forms was developed. The synthesis of the used N, S-CQDs dots was achieved using a simple and cost-effective process, as it used widely attainable starting materials (CA and TSC) in a one-step hydrothermal process to produce a highly water soluble, excellent biocompatible sensor with a size less than 10 nm. The characterization of the produced N, S-CQDs was performed using different techniques including HRTEM, UV-vis absorption spectroscopy, fluorescence spectroscopy, in addition to FT-IR. The studied drugs quantitatively quenched the fluorescence of the fabricated sensor based on the dynamic quenching mechanism resulting in rapid and long-lasting fluorescence response. The developed method was sensitive, accurate, and precise with wide linearity range of 2.0–25.0 μM, 10.0–100.0 μM and 20.0–200.0 μM for PRX, TNX and LRX, respectively. The suggested approach was adapted for the estimation of PRX in spiked human plasma with accepted value of SD and good percent recoveries ranging from 97.95–101.36%. This is the first direct spectrofluorimetric approach for determining PRX, TNX or LRX that does not require previous derivatization or use of chromogenic reagent.

The proposed approach was carefully validated in accordance with ICH guidelines.

## Ethical approval

This article does not include any studies on human participants or animals carried out by any of the authors.

## Conflicts of interest

The authors declare that they have no conflict of interest.

## References

- 1 M. J. Molaei, *Anal. Methods*, 2020, **12**, 1266–1287.
- 2 S. Zhu, Y. Song, X. Zhao, J. Shao, J. Zhang and B. Yang, *Nano Res.*, 2015, **8**, 355–381.
- 3 S. Liu, J. Tian, L. Wang, Y. Zhang, X. Qin, Y. Luo, A. M. Asiri, A. O. Al-Youbi and X. Sun, *Adv. Mater.*, 2012, **24**, 2037–2041.
- 4 M. Kim, L. Adamska, N. F. Hartmann, H. Kwon, J. Liu, K. A. Velizhanin, Y. Piao, L. R. Powell, B. Meany and S. K. Doorn, *J. Phys. Chem. C*, 2016, **120**, 11268–11276.
- 5 D. Iannazzo, A. Pistone, M. Salamò, S. Galvagno, R. Romeo, S. V. Giofré, C. Branca, G. Visalli and A. Di Pietro, *Int. J. Pharm.*, 2017, **518**, 185–192.
- 6 L. P. McGuinness, Y. Yan, A. Stacey, D. A. Simpson, L. T. Hall, D. Maclaurin, S. Prawer, P. Mulvaney, J. Wrachtrup and F. Caruso, *Nat. Nanotechnol.*, 2011, **6**, 358–363.
- 7 F. Li, D. Yang and H. Xu, *Chem.-Eur. J.*, 2019, **25**, 1165–1176.
- 8 L. Li and T. Dong, *J. Mater. Chem.*, 2018, **6**, 7944–7970.
- 9 T. S. Atabaev, *Nanomaterials*, 2018, **8**, 342.
- 10 L. Lin, Y. Luo, P. Tsai, J. Wang and X. Chen, *TrAC, Trends Anal. Chem.*, 2018, **103**, 87–101.
- 11 M. El-Maghrabey, R. El-Shaheny, F. Belal, N. Kishikawa and N. Kuroda, in *Nanosensor Technologies for Environmental Monitoring*, ed. Inamuddin and A. M. Asiri, Springer International Publishing, Cham, 2020, pp. 491–516, DOI: [10.1007/978-3-030-45116-5\\_17](https://doi.org/10.1007/978-3-030-45116-5_17).
- 12 H. Wu, J. Jiang, X. Gu and C. Tong, *Microchim. Acta*, 2017, **184**, 2291–2298.

13 J. Zhou, P. Lin, J. Ma, X. Shan, H. Feng, C. Chen, J. Chen and Z. Qian, *RSC Adv.*, 2013, **3**, 9625–9628.

14 M. Xue, L. Zhang, M. Zou, C. Lan, Z. Zhan and S. Zhao, *Sens. Actuators, B*, 2015, **219**, 50–56.

15 J. Chen, J. Liu, J. Li, L. Xu and Y. Qiao, *J. Colloid Interface Sci.*, 2017, **485**, 167–174.

16 Y. Wang, Q. Zhuang and Y. Ni, *Chem.-Eur. J.*, 2015, **21**, 13004–13011.

17 D. Sun, R. Ban, P.-H. Zhang, G.-H. Wu, J.-R. Zhang and J.-J. Zhu, *Carbon*, 2013, **64**, 424–434.

18 M. Amjadi, J. L. Manzoori, T. Hallaj and N. Azizi, *J. Lumin.*, 2017, **182**, 246–251.

19 L. S. Goodman, *Goodman and Gilman's the Pharmacological Basis of Therapeutics*, McGraw-Hill, New York, 1996.

20 M. Guttaduria, *Acta Obstet. Gynecol. Scand.*, 1986, **65**, 11–13.

21 R. D. Howland, M. J. Mycek, R. A. Harvey and P. C. Champe, *Lippincott's Illustrated Reviews: Pharmacology*, Lippincott Williams & Wilkins, Philadelphia, 2006.

22 E. R. M. Hackmann, E. A. dos Santos Gianotto and M. I. R. M. Santoro, *Anal. Lett.*, 1993, **26**, 259–269.

23 S. N. H. Azmi, B. Iqbal, M. A. M. Jaboob, W. A. S. Al Shahari and N. Rahman, *J. Chin. Chem. Soc.*, 2009, **56**, 1083–1091.

24 A. S. Amin, *J. Pharm. Biomed. Anal.*, 2002, **29**, 729–736.

25 M. El-Ries, *Anal. Lett.*, 1998, **31**, 793–807.

26 J. L. Manzoori and M. Amjadi, *Microchim. Acta*, 2003, **143**, 39–44.

27 A. B. Tabrizi, *J. Food Drug Anal.*, 2007, **15**, 242–248.

28 M. Gamal, H. M. Ali, S. M. Fraihat and T. S. Elnasr, *Luminescence*, 2019, **34**, 644–650.

29 A. Feizollahi, A. A. Rafati, P. Assari and R. A. Joghani, *J. Electrochem. Soc.*, 2020, **167**, 067521.

30 G. Ghobadpour, F. Farjami and F. Fasihi, *Curr. Pharm. Anal.*, 2019, **15**, 45–50.

31 A. G. Dal, Z. Oktayer and D. Doğrukol-Ak, *J. Anal. Methods Chem.*, 2014, **2014**, 1–7.

32 J. Otarola, A. G. Lista, B. F. Band and M. Garrido, *J. Pharm. Anal.*, 2015, **5**, 70–73.

33 A. Chaplenko, O. Monogarova and K. Oskolok, *Int. J. Pharm. Biol. Arch.*, 2018, **9**, 31–35.

34 A. K. Singh, P. López García, F. P. Gomes, E. R. M. Kedor-Hackmann and M. I. R. M. Santoro, *Rev. Bras. Cienc. Farm.*, 2007, **43**, 615–622.

35 E. A. Taha, N. N. Salama and L. E.-S. A. Fattah, *Chem. Pharm. Bull.*, 2006, **54**, 653–658.

36 P. Antonoaea, A. G. Cárje, A. Ciurba, N. Todoran, A. R. Vlad and D. L. Muntean, *Acta Med. Marisiensis*, 2017, **63**, 178–182.

37 M. A. Madni, A. Raza, S. Abbas, N. Tahir, M. Rehman, P. M. Kashif and M. I. Khan, *Acta Pol. Pharm.*, 2016, **73**, 1129–1134.

38 M. Sadikoglu and A. Cabuk, *Int. J. Electrochem. Sci.*, 2019, **14**, 4508–4519.

39 A. Fatma and A. Sena, *Turk. J. Pharm. Sci.*, 2019, **16**, 184.

40 J. A. Balfour, A. Fitton and L. B. Barradell, *Drugs*, 1996, **51**, 639–657.

41 S. K. Sahoo, R. K. Giri, S. V. Patil, A. R. Behera and R. Mohapatra, *Trop. J. Pharm. Res.*, 2012, **11**, 269–273.

42 S. N. H. Shah, K. Sohail, Z. Javaid, M. Zaman and E. Basheer, *Pak. J. Pharm. Sci.*, 2019, **32**, 333–338.

43 F. Belal, M. A. Omar, S. M. Derayea, S. Zayed, M. A. Hammad, S. F. Saleh, H. A. Alhazmi and M. Al Bratty, *Curr. Pharm. Anal.*, 2020, **16**, 1148–1156.

44 N. Salunkhe, N. Jadhav and S. Bhinge, *Sep. Sci. Plus*, 2019, **2**, 405–415.

45 M. Ghoneim, A. Beltagi and A. Radi, *Anal. Sci.*, 2002, **18**, 183–186.

46 B. Bozal and B. Uslu, *Comb. Chem. High Throughput Screening*, 2010, **13**, 599–609.

47 G. Magdy, A. F. A. Hakiem, F. Belal and A. M. Abdel-Megied, *Food Chem.*, 2021, **343**, 128539.

48 F. Belal, M. Mabrouk, S. Hammad, A. Barseem and H. Ahmed, *J. Fluoresc.*, 2021, **31**, 85–90.

49 X. Wang, L. Cao, S. T. Yang, F. Lu, M. J. Meziani, L. Tian, K. W. Sun, M. A. Bloodgood and Y. P. Sun, *Angew. Chem., Int. Ed.*, 2010, **49**, 5310–5314.

50 P. Anilkumar, X. Wang, L. Cao, S. Sahu, J.-H. Liu, P. Wang, K. Korch, K. N. Tackett II, A. Parenzan and Y.-P. Sun, *Nanoscale*, 2011, **3**, 2023–2027.

51 Z. Fu and F. Cui, *RSC Adv.*, 2016, **6**, 63681–63688.

52 M. Xue, L. Zhang, Z. Zhan, M. Zou, Y. Huang and S. Zhao, *Talanta*, 2016, **150**, 324–330.

53 L. Hu, Y. Sun, Y. Zhou, L. Bai, Y. Zhang, M. Han, H. Huang, Y. Liu and Z. Kang, *Inorg. Chem. Front.*, 2017, **4**, 946–953.

54 S. O. A. Ahmad, M. Ikram, M. Imran, S. Naz, A. Ul-Hamid, A. Haider, A. Shahzadi and J. Haider, *RSC Adv.*, 2021, **11**, 23330–23344.

55 S. Mureed, S. Naz, A. Haider, A. Raza, A. Ul-Hamid, J. Haider, M. Ikram, R. Ghaffar, M. Irshad and A. Ghaffar, *Nanoscale Res. Lett.*, 2021, **16**, 1–12.

56 M. Ikram, I. Hussain, J. Hassan, A. Haider, M. Imran, M. Aqeel, A. Ul-Hamid and S. Ali, *Ceram. Int.*, 2020, **46**, 21073–21083.

57 A. Haider, M. Ijaz, S. Ali, J. Haider, M. Imran, H. Majeed, I. Shahzadi, M. M. Ali, J. A. Khan and M. Ikram, *Nanoscale Res. Lett.*, 2020, **15**, 1–11.

58 J. Tashkhourian, G. Absalan, M. Jafari and S. Zare, *Spectrochim. Acta, Part A*, 2016, **152**, 119–125.

59 J. R. Lakowicz, *Principles of Fluorescence Spectroscopy*, Springer Science & Business Media, 2013.

60 V. D. Suryawanshi, L. S. Walekar, A. H. Gore, P. V. Anbhule and G. B. Kolekar, *J. Pharm. Anal.*, 2016, **6**, 56–63.

61 G. Xiang, C. Tong and H. Lin, *J. Fluoresc.*, 2007, **17**, 512–521.

62 K. Grigoryan and A. Ghazaryan, *Chem. Biol.*, 2013, **2**, 6–10.

63 Y.-h. Zhang, H.-s. Zhang, X.-f. Guo and H. Wang, *Microchem. J.*, 2008, **89**, 142–147.

64 ICH Harmonised Tripartite Guidelines, *Validation of analytical procedures: text and methodology Q2 (R1)*, <https://www.ich.org/products/guidelines/quality/article/quality-guidelines.html>, accessed, April, 2022.

65 J. Miller and J. Miller, *Statistics and Chemometrics for Analytical Chemistry*, Prentice Hall, Hariow, England, 2005.

66 D. C. Hobbs and T. M. Twomey, *J. Clin. Pharmacol.*, 1979, **19**, 270–281.

67 A. C. Moffat, M. D. Osselton, B. Widdop and J. Watts, *Clarke's Analysis of Drugs and Poisons*, Pharmaceutical Press, London, 2011.

